Available online at www.sciencedirect.com
ScienceDirect
Trans. Nonferrous Met. Soc. China 19(2009) 517−524
Transactions of Nonferrous Metals Society of China
www.tnmsc.cn

Comparison of corrosion behaviors of AZ31, AZ91, AM60 and ZK60 magnesium alloys

CHENG Ying-liang(程英亮)[1], QIN Ting-wei(秦廷伟)[1], WANG Hui-min(王慧敏)[1], ZHANG Zhao(张 昭)[2]

1. College of Materials Science and Engineering, Hunan University, Changsha 410082, China;
2. Department of Chemistry, Zhejiang University, Hangzhou 310027, China

Received 17 September 2008; accepted 6 December 2008

Abstract: The corrosion behaviours of four kinds of rolled magnesium alloys of AZ31, AZ91, AM60 and ZK60 were studied in 1 mol/L sodium chloride solution. The results of EIS and potentiodynamic polarization show that the corrosion resistance of the four materials is ranked as ZK60＞AM60＞AZ31＞AZ91. The corrosion processes of the four magnesium alloys were also analyzed by SEM and energy dispersive spectroscopy(EDS). The results show that the corrosion patterns of the four alloys are localized corrosion and the galvanic couples formed by the second phase particles and the matrix are the main source of the localized corrosion of magnesium alloys. The corrosion resistance of the different magnesium alloys has direct relationship with the concentration of alloying elements and microstructure of magnesium alloys. The ratio of the β phase in AZ91 is higher than that in AZ31 and the β phase can form micro-galvanic cell with the alloy matrix, as a result, the corrosion resistance of AZ31 will be higher than AZ91. The manganese element in AM60 magnesium alloy can form the second phase particle of AlMnFe, which can reduce the Fe content in magnesium alloy matrix, purifying the microstructure of alloy, as a result, the corrosion resistance of AM60 is improved. However, due to the more noble galvanic couples of AlMnFe and matrix, the microscopic corrosion morphology of AM60 is more localized. The zirconium element in ZK60 magnesium alloy can refine grain, form stable compounds with Fe and Si, and purify the composition of alloy, which results in the good corrosion resistance of ZK60 magnesium alloy.
Key words: magnesium alloy; corrosion; electrochemical impedance spectrum; polarization curves

1 Introduction

Magnesium is the lightest structural metal. Compared with steel, aluminum alloys and engineering plastics, magnesium alloys possess many excellent properties, such as light mass, high specific strength, high thermal conductivity and electromagnetic interference resistance[1−3]. But so far, their application is limited due to the poor corrosion resistance. Magnesium will corrode in most inorganic acidic and neutral solutions; and the corrosion rate is usually high [4−12].

The corrosion reactions of magnesium alloy and pure magnesium are similar in neutral and alkaline media and the overall reaction[13] can be expressed as

$$Mg+2H_2O=Mg(OH)_2+H_2 \quad (1)$$

However, the reaction formula is a general description and doesn't reveal some basic and crucial steps of the corrosion process of magnesium alloys. And the formula cannot explain a common phenomenon in the anodic dissolution process of magnesium alloys, that is, the negative differential effects(NDE). In order to explain the NDE phenomenon, a variety of mechanisms have been proposed[14−17], but they all have their own limitations and cannot explain all of the experimental facts.

The corrosion property of magnesium alloy is closely related to its high chemical activity and the contents of impurities. Mg-Al alloy is the most common category of magnesium alloy and there are many different versions about the influence of aluminum on the corrosion resistance of magnesium alloy. LUNDER et al[18] considered that when the content of aluminum reaches 8% (mass fraction), the corrosion resistance of magnesium alloy could be greatly improved. However, the study with TEM by WARNER et al[19] indicated that 5% Al in magnesium alloy was helpful for the corrosion resistance[19]. HEHMANN et al[20] studied the corrosion behavior of magnesium alloys with aluminum

Foundation item: Foundation item: Project(50471043) supported by the National Natural Science Foundation of China
Corresponding author: CHENG Ying-liang; Tel: +86-731-8821610; E-mail: chengyl@hnu.cn; deepblacksea@163.com
DOI: 10.1016/S1003-6326(08)60305-2

content of 9.0%−62.3% and concluded that aluminum content from 9.6% to 23.4% was beneficial to improving the corrosion resistance of magnesium alloy. Similarly, the controversial view on the role of the β phase (intermetallic compounds $Mg_{17}Al_{12}$) in the microstructure of AZ series magnesium alloy still exists. It is generally thought that in the corrosion of magnesium alloys, the β phase acts as cathode and it has good passive behavior in broad pH ranges. After the dissolution of the anodic α phase (the matrix), the β phase may play the role of a barrier layer to inhibit corrosion. However, according to the previous studies [21−22], the role of β phase in corrosion process was related to its content, size and distribution. When the mass fraction of β phase is high, the grain size of magnesium alloy is small, and the β phase distributes continuously on the matrix α phase, so it may play the role of a barrier layer to deter corrosion. On the contrary, if the grain size is larger and the distance between β phases is enlarged, galvanic corrosion may occur and cause the decline of the corrosion resistance.

Generally, aluminum and zirconium are main alloying elements of magnesium alloys. Alloying elements have an influence on the mechanical, physical and chemical properties of magnesium alloy. Aluminum is the most important alloying element and can significantly improve the tensile strength by the formation of $Mg_{17}Al_{12}$ phase. The elements of Zn and Mn in magnesium alloys have a similar role to Al. The solubility of Zr in magnesium is lower and Zr has strong affinity with oxygen, so it can form zirconia to refine the grain size of magnesium alloys. Manganese can improve the corrosion resistance of Mg-Al alloy and Mg-Al-Zn alloy by removing iron and other heavy metal elements to avoid the formation of harmful intermetallic compounds. Besides, manganese can refine grain size and improve welding properties of magnesium alloys. But up to now, there are relatively little studies about the influence of different alloying elements on the electrochemical corrosion behavior of magnesium alloys. In this work, the corrosion processes of AZ31, AZ91, AM60 and ZK60 are studied by electrochemical techniques, SEM and EDS to reveal the effects of different alloying elements.

2 Experimental

The materials used for this experiment were rolled magnesium alloy plates of AZ31, AZ91, AM60 and ZK60. Table 1 presents their chemical compositions. Samples were cut into squares with a dimension of 10 mm×10 mm. All samples were connected with copper wire and then enveloped by epoxy resin with only an exposed area of 1 cm^2 as the working electrode. Before experiments, the working electrode was successively polished with 600-grit, 1 200-grit abrasive paper and 2.5 μm diamond paste, then carefully degreased with acetone and rinsed with distilled water, finally dried in a stream of warm air. Electrochemical tests were carried out in 1 mol/L NaCl solution using electrochemical impedance spectroscopy(EIS) and potentiodynamic polarization techniques. All experiments were performed in a thermostated container at a fixed temperature of 25 ℃. The cell setup was composed of a three-electrode system with saturated calomel electrode(SCE) used as reference electrode, a large platinum sheet as auxiliary electrode, and the sample as the working electrode. Before EIS and potentiodynamic polarization measurement, the working electrodes were immersed in NaCl solution for the stability. EIS was obtained at the open circuit potential (OCP) from 10 000 to 0.005 Hz with a perturbative voltage amplitude of 5 mV.

Table 1 Chemical compositions of magnesium alloys (mass fraction, %)

Alloy	Al	Mn	Zn	Zr	Mg
AZ31	3.0	0.20	1.0	−	Bal.
AZ91	9.0	0.13	0.7	−	Bal.
AM60	6.0	0.13	−	−	Bal.
ZK60	−	−	5.5	0.45	Bal.

Besides the electrochemical tests, the surface morphologies of AZ31, AZ91, AM60 and ZK60 immersed in 1 mol/L NaCl solution for different times were examined by a JEOL JSM−6700F scanning electron microscope(SEM). The samples were first abrased by 600- and 1 200-grit abrasive paper and finally polished with 2.5 μm diamond paste, then the samples were cleaned by distilled water and acetone. Finally, the samples were sealed by wax with the working surface exposed only and immersed in a solution of 1 mol/L NaCl at constant temperature of 25 ℃. After 1 h and 8 h, the samples were taken out and examined by SEM. The corrosion products on the samples were cleaned ultrasonically in distilled water for the surface observation.

3 Results and discussion

3.1 Potentiodynamic polarization curves

Fig.1 shows the results of the potentiodyamic polarization tests for the four alloys and the scan rate of the tests is 1 mV/s.

The free corrosion current densities (J_{corr}) in Fig.1 are calculated and listed in Table 2. It is indicated that the J_{corr} is ranked as ZK60＜AM60＜AZ31＜AZ91. It is

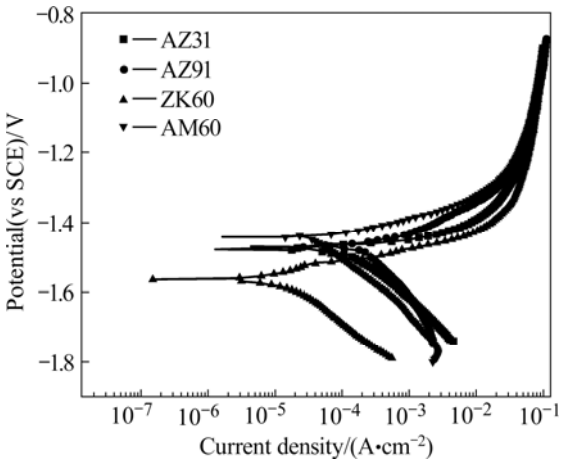

Fig.1 Potentiodynamic curves for four magnesium alloys in 1 mol/L NaCl

Table 2 Free corrosion current densities (J_{corr}) of four magnesium alloys

Alloy	J_{corr}/(A·cm^{-2})
AZ91	4.886×10^{-4}
AZ31	2.349×10^{-4}
AM60	1.567×10^{-4}
ZK60	1.003×10^{-5}

well known that the free corrosion current density is correlated with the corrosion resistance of metals. The less the free corrosion current density, the higher the corrosion resistance. It can be acquired from this experiment that the corrosion resistance of ZK60 is the best and that of AZ91 is the worst.

3.2 Results of electrochemical impedance spectroscopy

EIS is a technique with small perturbative signal and the surface damage of the sample is very little. Besides, the corrosion mechanism can be estimated by analyzing the measured electrochemical impedance spectrum. In this experiment, the immersion of the four magnesium alloys was carried out continuously in 1 mol/L NaCl solution and the EIS results at different immersion times (0.5 h, 2 h, 4 h and 8 h) are given in Fig.2.

It can be seen from Fig.2 that these diagrams include a low-frequency inductive loop. For AZ31, AZ91 and AM60, the diagrams contain two time constants in high and medium regions because there are two arcs in the Nyquist plots. The low-frequency inductive loop may arise from the partial protection of the surface oxide film,

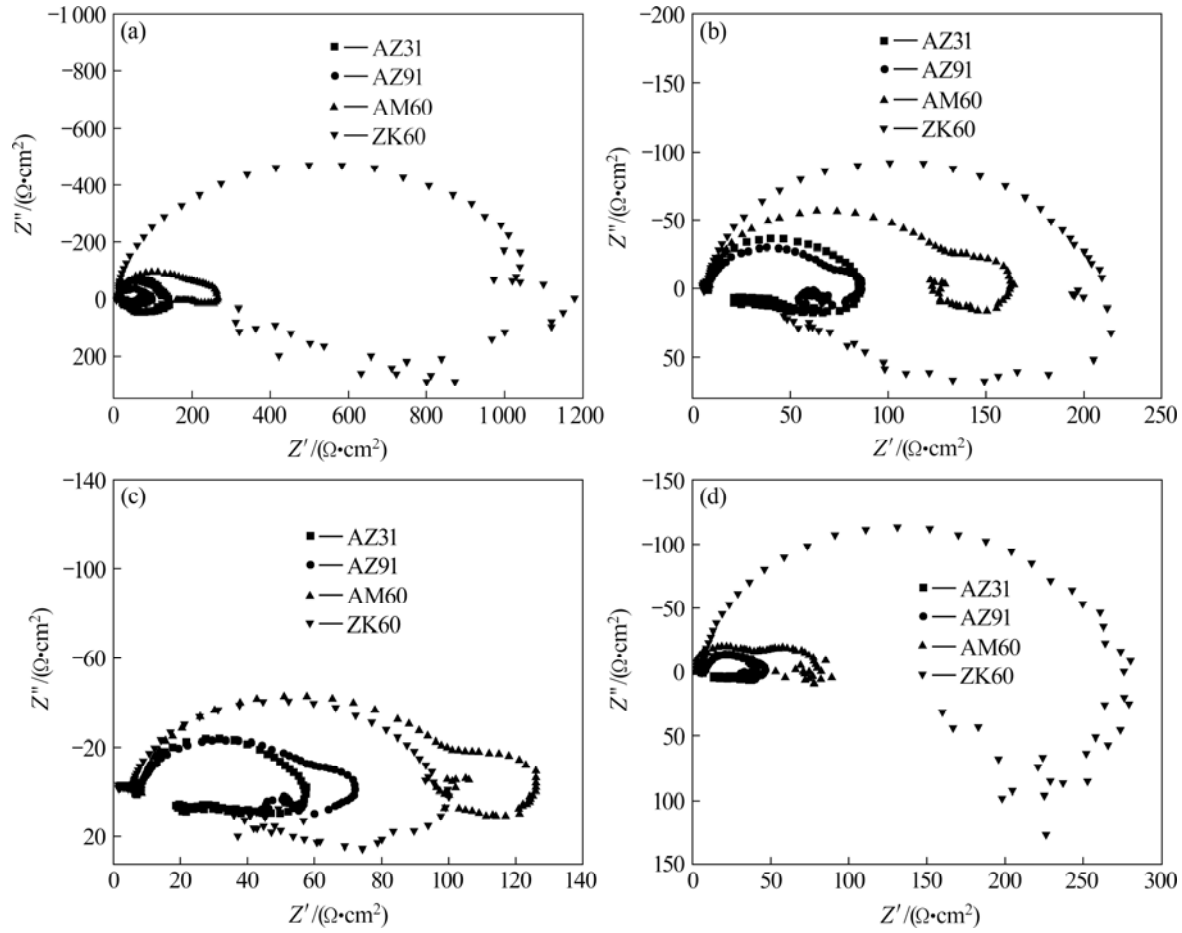

Fig.2 Nyquist plots of four magnesium alloys at different immersion time: (a) 0.5 h; (b) 2 h; (c) 4 h; (d) 8 h

which can be explained by Cao's model including one state variable apart from electrode potential[23].

According to Cao's theory, if the electrode reaction only contains a state variable apart from electrode voltage, the Faraday admittance of the electrode/solution interface can be expressed as

$$Y=j\omega C_{dl}+1/R_{ct}+(\partial I_F/\partial X)(dX/dE)/[1-j\omega/(\partial X'/\partial X)] \quad (2)$$

where Y is admittance; ω is angular frequency; C_{dl} is the capacitance of the double layer; R_{ct} is the charge transfer resistance; I_F is Faradaic current; X is state variable; and $X'=dX/dt$.

The former two parts at the right side of Eq.(2) corresponds to the high-frequency part of Fig.2 while the last one contributes to the low-frequency part.

When $(\partial I_F/\partial X)(dX/dE)>0$, the inductive loop will appear at the low frequency part of the electrochemical impedance spectrum. It is believed that there are partly protective oxide films on magnesium alloys in neutral and alkaline solutions[24]. In this experiment, the state variable of the electrode surface is the percentage of coverage(θ) of the oxide film on magnesium alloy. The increase of electrode potential may result in the breakage of the film, therefore, $(d\theta/dE)<0$, which means that the percentage of coverage(θ) of the oxide film reduces with the increase of potential. In addition, the anodic current will result in the partial dissolution of oxide film, so the percentage of coverage(θ) of electrode surface decreases with the increase of anodic current, which means $(\partial I_F/\partial\theta)<0$. As a result, $(\partial I_F/\partial X)(d\theta/dE)>0$ is obtained in this circumstance.

According to Cao's theory, inductive reactance will occur at the low-frequency range. The charge transfer resistance (R_{ct}) can be acquired from the high-frequency range in Fig.2. It corresponds to the dissolution of magnesium alloy and can directly characterize the corrosion resistance of the samples. The relationship of the R_{ct} with immersion time is plotted in Fig.3 and it is used to compare the relationship of the corrosion process of different magnesium alloys with time.

Fig.3 shows that the order of the corrosion resistance for the four materials is ZK60＞AM60＞AZ31＞AZ91. This conclusion keeps highly consistent with the results of the potentiodynamic polarization curves. In the early corrosion stage, the corrosion resistance of ZK60 is much higher than that of the other magnesium alloys. At the immersion time of 0.5 h, the R_{ct} of ZK60 is 1 023.00 Ω·cm^2, while that of AZ91 is 77.21 Ω·cm^2. The former is almost 13 times the latter. High corrosion resistance of ZK60 is related to Zr element. In the early corrosion stage, the R_{ct} of AZ91 is less than that of AZ31, however, after 2 h, the two are very similar. But the R_{ct} of AM60 is always higher than that of AZ31 or AZ91.

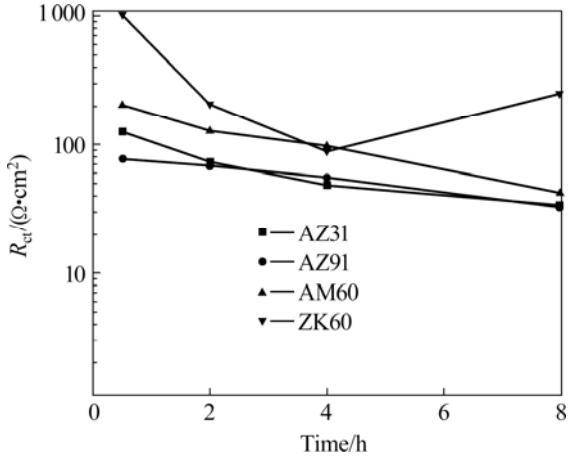

Fig.3 Variation of charge transfer resistance of four magnesium alloys with time

3.3 Morphology and corrosion resistance

The surface morphologies of AZ31, AZ91, AM60 and ZK60 immersed in 1 mol/L NaCl solution for 1 h and 8 h by scanning electron microscope(SEM) are shown in Fig.4 and Fig.5, respectively.

It can be seen in Fig.4 that there are plenty of visible corrosion products on the surface of AZ31 after 1 h immersion and some localized pits occur on the surface of AZ91. The surface corrosion states of AM60 and ZK60 are not as severe as those of AZ31 and AZ91. The SEM images indicate that the corrosion resistance of AM60 or ZK60 is higher than that of AZ31 or AZ91. This is consistent with the results of electrochemical impedance spectroscopy(EIS) and potentiodynamic polarization curves.

It is found in Fig.5 that the surface morphologies of four magnesium alloys exhibit localized corrosion morphology after 8 h immersion. Corrosion pits almost distribute on the entire surface of AZ31. There are two forms of surface morphology on the corrosion surface of AZ91. One side is highly corroded with the feature of trenches while the adjacent part is less severe. The corrosion morphology of AM60 is more localized; some obvious pits appear on the surface of AM60; and the other part is seldom corroded. The form of trench-like surface also appears on ZK60, however, the corrosion is less sever than other alloy.

The previous electrochemical results show that the order of corrosion resistance of four magnesium alloys in this experiment is ZK60＞AM60＞AZ31＞AZ91. SEM images of the corrosion immersion alloys also confirm this conclusion. The results may be caused by the different distribution of alloying elements in microscopic scale and the microstructure of alloys, which are the fundamental reasons for the metal corrosion morphology and corrosion resistance.

Fig.6 shows the backscattered electron image of

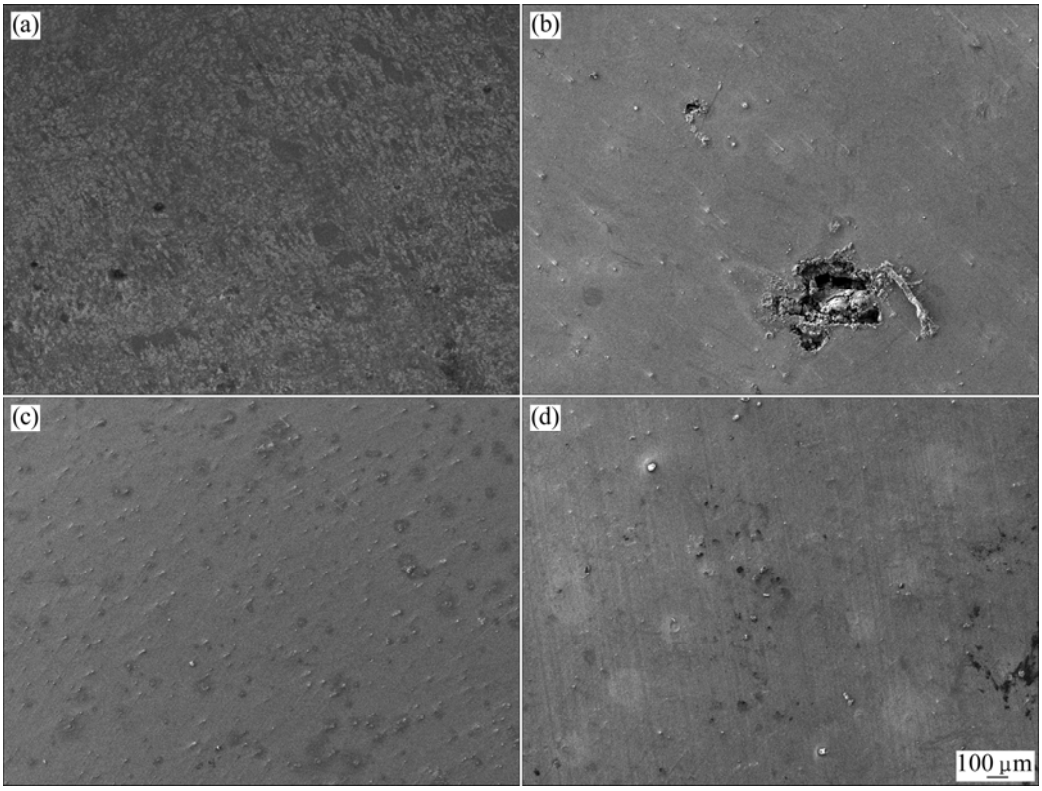

Fig.4 SEM surface morphologies of different magnesium alloys after 1 h immersion: (a) AZ31; (b) AZ91; (c) AM60; (d) ZK60

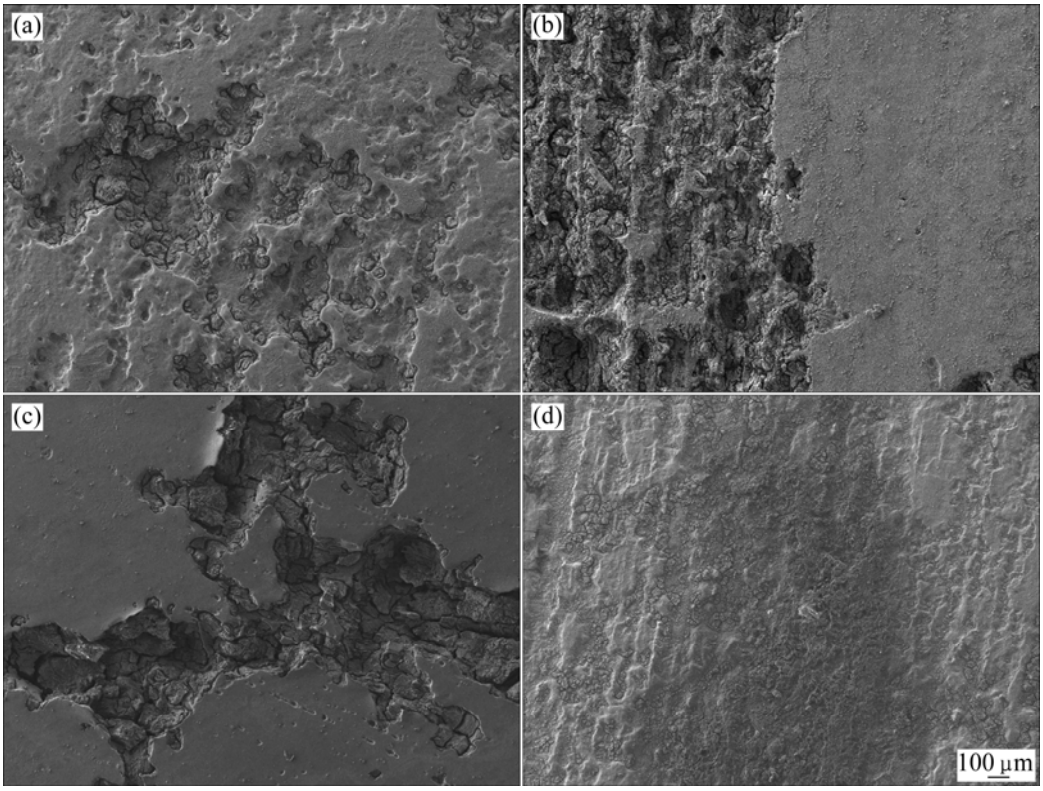

Fig.5 SEM surface morphologies of different magnesium alloys after 8 h immersion: (a) AZ31; (b) AZ91; (c) AM60; (d) ZK60

AZ91 magnesium alloy. There are a great number of the bright second-phase particles in the microstructure. The elemental compositions of the bright second-phase particles and the magnesium alloy matrix examined by EDS are listed in Table 3.

It is known from Table 3 that the content of Al in the bright second-phase particles reaches 23.87%, thus, it might be the β phase ($Mg_{17}Al_{12}$). The electrode potential

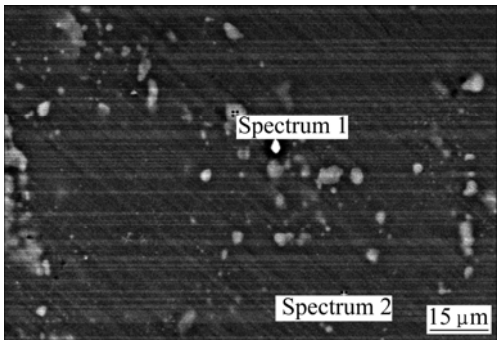

Fig.6 Backscattered electron image of AZ91 magnesium alloy

Table 3 EDS results of corresponding area as indicated in Fig.6 (mass fraction, %)

Element	Area 1	Area 2
C	6.35	6.46
O	1.35	1.69
Mg	66.88	86.61
Al	23.87	5.25
Zn	1.54	−
Total	100.00	100.00

of the β phase is higher than the matrix, therefore, it will form microcells with the adjacent matrix and accelerate the corrosion process. Because the Al content in AZ91 is higher than that of AZ31, the content of β phase of AZ91 will be higher than that of AZ31 and the number of corrosion microcells of AZ91 is also larger than that of AZ31, as a result, the corrosion resistance of AZ91 is lower than that of AZ31.

Fig.7 shows the backscattered electron image of AM60 and there are a few bright second-phase particles in alloy (as indicated by areas 1, 2 and 3). The elemental compositions of those locations are also examined by EDS, and the results are listed in Table 4.

The results in Table 4 indicate that the white second-phase corresponding to areas 1, 2 and 3 contains

Table 4 EDS results of corresponding areas in Fig.7 (mass fraction, %)

Element	Area 1	Area 2	Area 3	Area 4	Area 5
C	7.55	−	5.47	6.20	8.94
O	3.45	2.96	2.50	3.02	4.10
Mg	17.31	7.93	17.12	86.11	82.90
Al	42.06	44.09	36.33	4.18	4.06
Mn	20.05	42.68	33.31	−	−
Fe	9.58	1.60	4.23	−	−
Si	−	0.73	1.02	0.49	−
Total	100.00	100.00	100.00	100.00	100.00

Al, Mn and a relatively high concentration of iron, and this second-phase particle could be AlMnFe intermetallic. Areas 4 and 5 are the magnesium-based α-phase solid solutions. It is well-known that the inclusion of heavy metals such as iron and copper is one of the major reasons that cause the deterioration of the corrosion resistance of magnesium alloys. And by forming AlMnFe, the content of Fe in alloy can be reduced by precipitating with the slag and the grain size of alloys is refined[25]. It can be seen in Fig.5 that the corrosion morphology of AM60 alloy is more localized than the other alloys. This can be explained by the fact that the galvanic couples formed by AlMnFe and matrix is more noble than the other galvanic couples in other alloys (in AZ31 and AZ91, the galvanic couple is $Mg_{17}Al_{12}$ and matrix; in ZK60, the couple is MgZn and matrix; and AlMnFe has more noble electrode potential than $Mg_{17}Al_{12}$ and MgZn). Due to the fact that manganese can clean up the composition of matrix, the matrix of the AM60 is more purified. Accordingly, it is found from Figs.6−8 that the second phase particles of FeAlMn in AM60 are less than those in other alloys, as a result, the corrosion morphology of AM60 will be more localized.

Fig.8 shows the backscattered electron image of ZK60. Similarly, there are also a lot of bright irregular second-phase particles. The elemental compositions of the matrix and the second-phase particles examined by EDS are listed in Table 5.

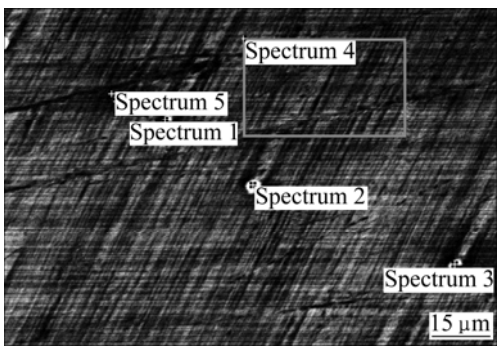

Fig.7 Backscattered electron image of AM60 magnesium alloy

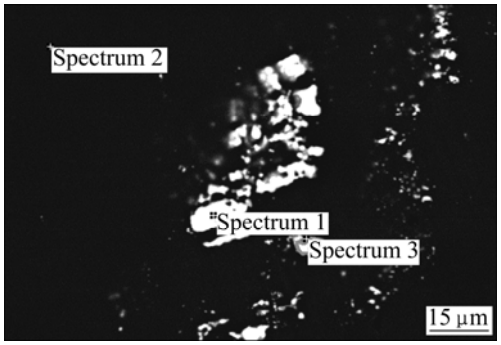

Fig.8 Backscattered electron image of ZK60 magnesium alloy

Table 5 EDS results of corresponding areas in Fig.8

Element	Area 1	Area 2	Area 3
C	21.74	12.05	8.04
O	2.87	2.30	2.43
Mg	21.55	82.29	43.88
Zn	53.84	3.36	45.64
Total	100.00	100.00	100.00

It is seen from Table 5 that the matrix is mainly magnesium-based α-phase solid solution containing 3.36%Zn (area 2), while the second-phase particles with high Zn content may be MgZn intermetallic compound. The corrosion morphology of ZK60 is also localized corrosion which may be the result of the formation of galvanic cells by the matrix and second phase particles. However, the electropotential of Zn is more negative and the galvanic coulpe formed by MgZn and matrix will be less noble. As a result, the corrosion morphology of ZK60 is less severe than AZ31 and AZ91 (see Fig.5). The content of zirconium cannot be detected by EDS. Zirconium can refine grain strongly and form stable compound with Fe and Si, purifying the alloy composition[25]. The best corrosion resistance of ZK60 shown by the electrochemical tests in this experiment may be caused by this reason.

4 Conclusions

1) The corrosion behaviours of four kinds of rolled magnesium alloy plates of AZ31, AZ91, AM60 and ZK60 are studied in 1 mol/L sodium chloride solution. The result of potentiodynamic polarization curves show that the J_{corr} of the four materials are ranked as AZ91＞AZ31＞AM60＞ZK60. The result of EIS shows that they have similar EIS diagrams containing a high-frequency capacitive loop and a low-frequency inductive loop. R_{ct} of the four materials are ranked as ZK60＞AM60＞AZ31＞AZ91. It is shown from both two techniques that the corrosion resistance of the four magnesium alloys are ranked as ZK60＞AM60＞AZ31＞AZ91.

2) The corrosion processes of the four magnesium alloys are also analyzed by SEM and energy dispersive spectroscopy(EDS). The results show that the corrosion pattern of the four alloys is localized corrosion. The galvanic couples formed by the second phase particles and the matrix are the main source of the localized corrosion of magnesium alloys; and the microscopic corrosion morphology of the alloys has strong relationship with the property and distribution of the second phase particles.

3) The aluminum content in AZ91 is higher than that in AZ31, thus the ratio of the β phase in AZ91 is higher than that in AZ31, and the β phase can form micro-galvanic cell with the alloy matrix, as a result, the corrosion resistance of AZ91 is lower than AZ31. The manganese element in AM60 magnesium alloy can form the second phase particle of AlMnFe, which can reduce the Fe content in magnesium alloy matrix, purifying the microstructure of alloy, as a result, the corrosion resistance of AM60 is improved. However, due to the more noble galvanic couple of AlMnFe and matrix, the microscopic corrosion morphology of AM60 is more localized. The zirconium element in ZK60 magnesium alloy can refine grain, form stable compounds with Fe and Si, and purify the composition of alloy, resulting in the good corrosion resistance of ZK60 magnesium alloy.

References

[1] DECKER R F. The renaissance in magnesium [J]. Advanced Materilas & Processes, 1998, 154(3): 31−33.

[2] THOMAS J R, DARRY L A. High ductility magnesium alloys in automotive applications [J]. Advanced Materials & Processes, 1994, 145(6): 28-32.

[3] FROES F H, ELIEZER D, AGHION E. The science, technology and application of magnesium [J]. Journal of the Minerals, Metals and Materials Society, 1998, 5(9): 30−34.

[4] MAKAR G L, KRUGER J. Corrosion of magnesium [J]. International Materials Reviews, 1993, 38(3): 138−153.

[5] RUDD A L, BRESLIN C B, MANSFELD F. The corrosion protection afforded by rare earth conversion coatings applied to magnesium [J]. Corrosion Science, 2000, 42(2): 275−288.

[6] SONG G L, JOHANNESSON B, HAPUGODA S, St JOHN D. Galvanic corrosion of magnesium alloy AZ91D in contact with an aluminium alloy, steel and zinc [J]. Corrosion Science, 2004, 46(4): 955−977.

[7] SONG Guang-ling, St JOHN D. Corrosion behaviour of magnesium in ethylene glycol [J]. Corrosion Science, 2004, 46(6): 1381−1399.

[8] SONG G L, BOWLES A L, St JOHN D H. Corrosion resistance of aged die cast magnesium alloy AZ91D [J]. Materials science and engineering, 2004, A366: 74−86.

[9] HUO Hong-wei, LI Ying, WANG Fu-hui. Corrosion of AZ91D magnesium alloy with a chemical conversion coating and electroless nickel layer [J]. Corrosion Science, 2004, 46(6): 1467−1477.

[10] CHIU L H, CHEN C C, YANG C F. Improvement of corrosion properties in an aluminum-sprayed AZ31 magnesium alloy by a post-hot pressing and anodizing treatment [J]. Surface and Coatings Technology, 2005, 191(2/3): 181−187.

[11] ZHANG Yong-jun, YAN Chuan-wei, WANG Fu-hui, LI Wen-fang. Electrochemical behavior of anodized Mg alloy AZ91D in chloride containing aqueous solution [J]. Corrosion Science, 2005, 47(11): 2816−2831.

[12] GUO X W, DING W J, LU C, ZHAI C Q. Inflence of ultrasonic power on the structure and composition of anodizing coatings formed on Mg alloys [J]. Surface and Coatings Technology, 2004, 183(2/3): 359−368.

[13] HUO H W, LI Y, WANG H N, WANG F H. The corrosion and protection of magnesium alloys [J]. Materials Review, 2001, 15(7):

25−27.

[14] MAKAR G L, KRUGER J. Corrosion studies of rapidly solidified magnesium alloys [J]. Journal of the Electrochemical Society, 1990, 137(2): 414−421.

[15] PERRAULT G G. Potentiostatic study of the magnesium electrode in aqueous solution [J]. J Electroanalytical Chemistry and Interfacial Electrochemistry, 1970, 27(1): 47−58.

[16] SONG Guang-ling, ATRENS A, St JOHN D, NAIRN J, LI Ying. The electrochemical corrosion of pure magnesium in 1 N NaCl [J]. Corrosion Science, 1997, 39(5): 855−875.

[17] LI Y, SONG G L, LIN H C, CAO C N. Study on the relationship between the corrosion interface structure and negative difference effect for pure magnesium [J]. Corrosion Science and Protection Technology, 1999, 11(4): 202−208.

[18] LUNDER O, LEIN J E, AUNE T K, NISANCIOGLU K. The role of magnesium aluminuim ($Mg_{17}Al_{12}$) phase in the corrosion of magnesium alloy AZ91 [J]. Corrosion, 1989, 45: 741−748.

[19] WARNER T J, THORNE N A, NUSSBAUM G, STOBBS W M. A cross sectional TEM study of corrosion initiation in rapidly solidified magnesium-based ribbon [J]. Surface and Interface Analysis, 1992, 19: 386−392.

[20] HEHMANN F, FROES F H, YOUNG W. Rapid solidification of alumium, magnesium, and titanium [J]. Journal of Metals, 1987, 39(8): 14−21.

[21] SONG G L, ANDREJ A, MATTHEW D. Influence of microstructure on the die cast AZ91D [J]. Corrosion Science, 1999, 41(2): 249−273.

[22] SONG G L, ANDREJ A, WU X L, ZHANG B. Corrosion behaviour of AZ21, AZ501 and AZ91 in sodium chloride [J]. Corrosion Science, 1998, 40(10): 1769−1791.

[23] CAO Chu-nan, ZHANG Jian-qing. An introduction to electrochemical impedance spectroscopy [M]. Beijing: Science Press, 2002: 26. (in Chinese)

[24] SONG Guang-ling, ATRENS A, St JOHN D, WU X, NAIRN J. The anodic dissolution of magnesium in chloride and sulphate solutions [J]. Corrosion Science, 1997, 39(10/11): 1981−2004.

[25] CHEN Zhen-hua. Magnesium alloys [M]. Beijing: Chemical Industry Press, 2004: 36. (in Chinese)

(Edited by YANG Bing)